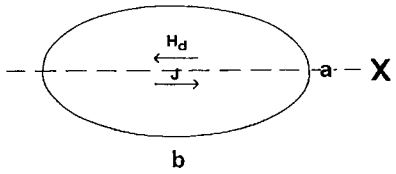

Fig. 1. Polarization and demagnetizing field in ellipsoid.

where q is the charge enclosed in e.s.u. This proof is inapplicable to magnetism because the equivalent formula is

$$\int_s B_n ds = 0 \qquad (2)$$

Page and Adams[4] deduce that the field outside a long thin magnet with approximately point poles is inversely proportional to μ_r, but from the nature of the approximations it is unlikely that this result holds for other shapes of magnet.

An illuminating example is provided by an ellipsoid with uniform polarization J in the X direction, as shown in Fig. 1. There is then a uniform demagnetizing field H_d inside the ellipsoid and using the Kennelly convention

$$B = J - \mu_0 H_d \qquad (3)$$

The field H at any external point and the demagnetizing field H_d inside the ellipsoid can be calculated by integrating contributions from dipoles in small elements of volume throughout the ellipsoid, although sometimes the mathematics is simplified by using an equivalent distribution of poles on elements of surface of the ellipsoid. Whether the field is being calculated inside or outside the ellipsoid, the correct result is given by the free space formula independently of the relative permeability of the ellipsoid.

Now the Kennelly formulation requires that the field due to a point pole or dipole is inversely proportional to μ_r, when the ellipsoid is immersed in a medium. As a constant, $1/\mu_r$ can be taken outside the integral and therefore applies to the whole ellipsoid. Thus at any point outside the ellipsoid H is reduced by $1/\mu_r$ and $B = \mu_0\mu_r H$ is unchanged. In particular this is true for an axial point a and an equatorial point b. Now at an equatorial point b, H is tangential to the surface of the ellipsoid and is therefore continuous across the boundary. So H_d is also reduced by the factor $1/\mu_r$. Inside the ellipsoid H_d is uniform, so H_d is also reduced by the factor $1/\mu_r$ at the axial point a just inside the ellipsoid. From equation (3), therefore, if J is unchanged, as is certainly possible in a hard magnetic material, B is increased by $H_d(1 - 1/\mu_r)$. Because B is normal to the surface of the ellipsoid at a and is continuous across the boundary, B is also increased outside the ellipsoid at a. Hence using the Kennelly formulation and the continuity relations, two contradictory results have been deduced. Outside the ellipsoid at an axial point a: (i) B is unchanged by a medium; (ii) B is increased by a medium. A similar reduction *ad absurdum* can be applied to the Sommerfeld convention.

The conclusion seems to be that we should not expect to find that the B and H produced by a magnet in a medium are simple functions of μ_r. They are more probably complicated functions of μ_r and geometrical factors depending on the shape of the magnet.

When a magnet is placed in a medium new dipoles are induced in the medium and those inside the magnet may or may not be altered. In general B and H can be calculated by taking account of all the macroscopic currents and magnetic dipoles that are near enough to be effective, using only the free space formulae.

This process would often be complicated, but the use of a formula involving μ_r or $1/\mu_r$ only as a simple coefficient is justified only when it leads to the same result. For the purpose of calculating B, H or magnetic forces (although not, of course, for some phenomena such as gyromagnetism), it does not matter whether magnetic dipoles are spinning electrons or orbiting electrons. It is entirely a matter of mathematical convenience whether we treat them as dipoles or small current loops.

We may not, however, replace a magnet by a single solenoid, when we are considering conditions inside the magnet. These depend on the magnet consisting of many interacting dipoles or current loops. This interaction is lost if we postulate a single solenoid to represent the magnet.

In conclusion, an explanation of the physical difference between B and H in a magnetic material may be of interest. The flux density B is measured by a coil encompassing the material and in general is due to three causes: (i) external causes, such as a current in a solenoid surrounding the material. (ii) The self-demagnetizing field originating from discontinuities at the boundaries of the material. (iii) The local polarization J.

The field H is that which influences J by altering the orientation of the individual dipoles or current loops. An individual dipole or current loop can exert no torque upon itself, so that J does not contribute to H and

$$H = (B - J)/\mu_0 \qquad (4)$$

I have constructed a model (yet to be published) consisting of a cubic array of small parallel magnets representing the atomic dipoles in a material. If one of these magnets is free to rotate, it turns so that it points in the opposite direction to the flux produced by the array as a whole, that is in the direction of H not B.

M. McCaig

Central Research Laboratory,
Permanent Magnet Association,
84 Brown Street, Sheffield, S1 1FA.

Received March 20; revised July 3, 1970.

[1] Stopes-Roe, H. V., *Nature*, **224**, 579 (1969).
[2] Rosser, W. G. V., *Nature*, **224**, 577 (1969).
[3] Starling, S. G., *Electricity and Magnetism*, 233 (Longmans Green and Co., London, 1921).
[4] Page, L. G., and Adams, N. I., *Principles of Electricity* (second ed.), 134 (D. van Nostrand Co. Inc., Toronto, New York and London, 1949).

Scattering of Gravitational Radiation by a Schwarzschild Black-hole

The discovery of pulsars and the general conviction that they are neutron stars resulting from gravitational collapse have strengthened the belief in the possible presence of Schwarzschild black-holes—or Schwarzschild horizons—in nature, the latter being the ultimate stage in the progressive spherical collapse of a massive star. The stability of these objects, which has been discussed in a recent report[1], ensures their continued existence after formation. Inasmuch as the infinite redshift associated with it and its behaviour as a one-way membrane make the

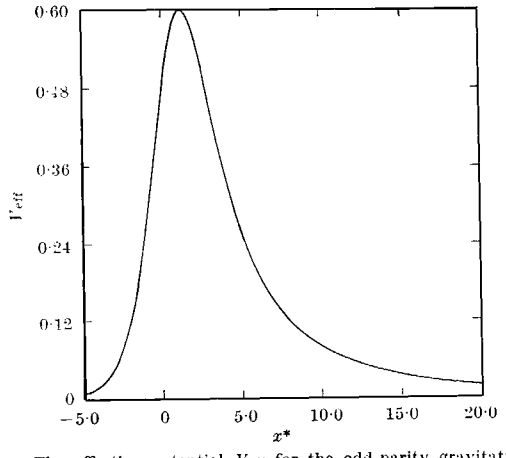

Fig. 1. The effective potential V_{eff} for the odd-parity gravitational waves of the lowest mode $l = 2$ plotted against x^*.

Schwarzschild horizon at once elusive and intriguing, it is important to explore theoretically all possible modes in which the presence of such a black-hole manifests itself. In what follows, we present a partial summary of some results obtained from an investigation of the scattering of gravitational waves by a Schwarzschild horizon.

To begin with, a spherically symmetric mass distribution is assumed to have collapsed into its Schwarzschild surface in the infinitely remote past. The scattering of gravitational waves by this configuration can be examined employing the perturbation techniques developed by Regge and Wheeler[2]. Retaining the notation of the authors and concentrating on the odd-parity waves, the perturbed Schwarzschild exterior line element in the Regge–Wheeler canonical gauge can be written as

$$ds^2 = -(1-2m/r)dt^2 + (1-2m/r)^{-1}dr^2 + r^2(d\theta^2 + \sin^2\theta\, d\varphi^2)$$
$$+ (h_0(r)\, dt\, d\varphi + h_1(r)\, dr\, d\varphi)\exp(-i\omega t)\sin\theta\, \frac{dP}{d\theta}\, l(\cos\theta)$$

where ω is the frequency of the gravitational waves. The Einstein empty-space field equations computed to first order in the perturbations[3] yield the following differential equations for the radial functions h_0 and h_1

$$\frac{d^2Q}{dx^{*2}} + (k^2 - V_{eff})Q = 0 \text{ with } V_{eff} = (1 - 1/x)\,(l(l+1)/x^2 - 3/x^3)$$

and

$$h_1 = \frac{i}{k}\,\frac{d}{dx^*}(xQ)$$

where we have defined

$x = r/2m$, $x^* = x + \ln(x-1)$, $k = 2m\omega$, and $Q = (1-1/x)h_1/x$

The exterior from $r = 2m$ to ∞ corresponds to the range of x^* from $-\infty$ to $+\infty$. The motion of the gravitational waves in this space is governed by the effective potential V_{eff} produced by the collapsed mass. The effective potential for the lowest possible mode $l = 2$ is plotted against x^* in Fig. 1, and the general behaviour of the potential for any higher value of l is the same, it is positive and goes to zero asymptotically as x^* approaches $\pm\infty$ and attains a maximum in between. From the Schrödinger form of the wave equation for Q and from the shape of the potential, it is evident that the scattering problem here is formally the same as that encountered in quantum mechanics for a one-dimensional potential barrier. A wave coming from spatial infinity is partially reflected by the effective potential, so that at large values of x we have both incoming and outgoing waves. On the other hand, as the Schwarzschild horizon acts as a sink for the radiation, there will be only waves entering the $r = 2m$ surface. Consequently the suitable asymptotic boundary conditions are $Q_\infty = A(k)e^{-ikx^*} + B(k)e^{+ikx^*}$ and $Q_\infty = C(k)e^{-ikx^*}$ for x^* approaching $\pm\infty$ respectively. In analogy with the quantum mechanical problem we can define the reflexion and transmission coefficients $R = |B/A|^2$ and $T = |C/A|^2$. A fraction R of the incident wave escapes to spatial infinity and is accessible to a distant observer, whereas a fraction T of the radiation is absorbed by the black-hole and thereby lost in the process. An analytical integration of the equation for Q leading to the computation of R and T has been impossible in practice and recourse had to be taken to numerical integration. This has been carried out—as have further computations to be discussed later—for the lowest mode $l = 2$ using a computer. Fig. 2 shows the plot of R against k^2. In the limit of zero frequency the reflexion coefficient approaches the limit 1 independent of the scattering mass, and so in this limit no information about the latter is forthcoming. Nevertheless, the rate at which the reflexion amplitude B/A, and so R, decreases as a function of the frequency should be perceptible when a sufficient range of frequencies is included and, because this rate clearly depends on the scattering mass, the presence of the latter is "coded" into the outgoing radiation. This leads us at once to the

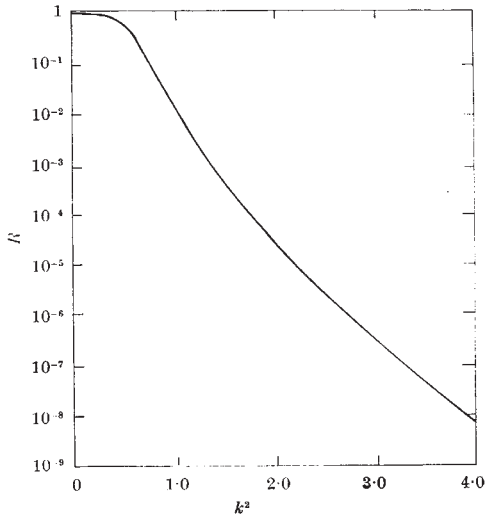

Fig. 2. The reflexion coefficient R as a function of k^2, the square of the frequency, for odd-parity mode $l = 2$.

physically more interesting phenomenon of the scattering of wave packets. By linear superposition we obtain an incoming wave packet at infinity with the spatial profile

$$\psi_{in}(x) = \int_{-\infty}^{+\infty} f(k)e^{-ikx}\, dk$$

and the corresponding outgoing or reflected packet

$$\psi_{out}(x) \int_{-\infty}^{+\infty} (B/A)\, f(k)e^{ikx}\, dk$$

The latter travels out without spreading and is received by the distant observer. We choose the Gaussian function

$$f(k) = \frac{1}{2\sqrt{\pi a}}\, e^{-k^2/4a}$$

in order to obtain a simple model for an incoming wave packet, that is, $\psi_{in} = e^{-ax^2}$. As the parameter a, which measures the width of the wave packet, is varied, some interesting features emerge. For low values of a ($a \lesssim 0{\cdot}01$), that is, for very broad incoming packets or equivalently for $f(k)$ sharply peaked at zero frequency, the reflected packet is practically unaffected. But, as the parameter a is gradually increased, ψ_{out} develops distinct maxima and minima that increase in number progressively, while their relative spacing undergoes a continuous change. As the parameter a, however, approaches approximately the value 1, that is, for a width of about the Schwarzschild radius, the process reaches a limit. Beyond this value of a, as the packet is made thinner, the outgoing packet will cease to develop new peaks and the relative spacing of these peaks will remain unaltered. In other words, any higher frequencies added to the original packet will have negligible effect on the scattered packet owing to their almost total absorption by the black-hole. As long as the incoming packet is spatially sharp enough, the reflected packet will manifestly carry information about the scattering mass. Fig. 3 shows an example of the "saturated" pattern corresponding to $a = 1$. The spacing between consecutive peaks and, consequently, the lag in their arrival times are measures of the scattering mass, as the spacing in the actual radial distance is given by $\Delta r = 2m\,\Delta x$.

The total energy carried by a wave packet $\psi(x)$ at spatial infinity can be computed by adapting a method used by Edelstein[4]. The result of this computation is that, for any mode l, the energy of the wave packet is given by

$$E = (c^5/32\pi G)\,(l-1)l(l+1)\,(l+2)\int(\psi(x))^2\, dx$$

where the integration is carried over the spatial extent of the wave packet. So the fraction of incident radiation scattered by the black-hole and reaching spatial infinity

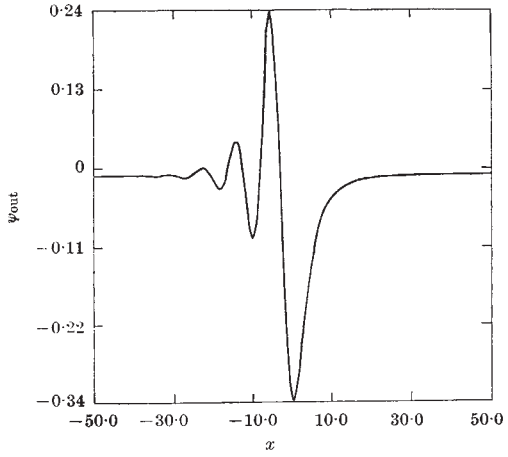

Fig. 3. The outgoing wave packet $\psi_{out}(x)$ at spatial infinity corresponding to the incident Gaussian wave packet $\psi_{in}(x)=e^{-ax^2}$ with $a=1$.

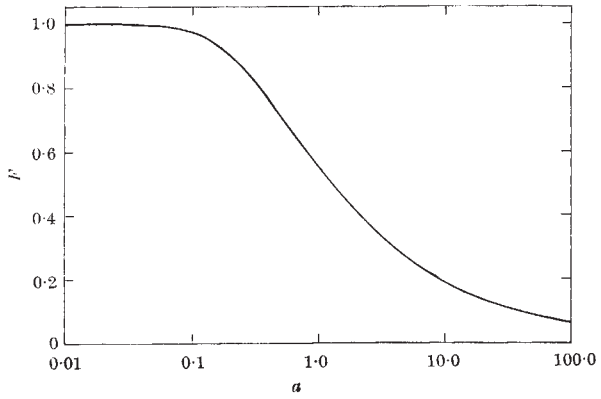

Fig. 4. The fraction F of the incident energy carried by the scattered outgoing wave packet at spatial infinity plotted as a function of the parameter a.

is the ratio of the energies carried by the incoming and the outgoing wave packets and is readily computed as

$$F=\frac{\int(\psi_{out})^2\,dx}{\int(\psi_{in})^2\,dx}=\left(\frac{2a}{\pi}\right)^{1/2}\int(\psi_{out})^2\,dx$$

In Fig. 4 the fraction F is plotted as a function of the width-parameter a. For an incident wave packet, the width of which is about a Schwarzschild radius ($a\simeq 1$) approximately half the total energy is scattered and the rest absorbed by the black-hole.

We have confined ourselves so far to some results concerning the scattering of odd-parity gravitational waves of angular momentum $l=2$ by a Schwarzschild black-hole. The mathematical and numerical details omitted here, as well as the scattering of higher l modes, even-parity waves, scalar gravitational waves and finally electromagnetic waves, will be discussed elsewhere in a separate and more detailed paper.

I thank Professor C. W. Misner for many helpful discussions, Dr A. Lapidus and Mr Gary Russel for their help in carrying out numerical computations, and the authorities of the NASA Institute for Space Studies, New York, for allowing me to use their computer. The research was supported by funds from the US National Science Foundation.

C. V. VISHVESHWARA

Department of Physics,
New York University,
251 Mercer Street,
New York, NY 10012.

Received June 10, 1970.

[1] Vishveshwara, C. V., *Phys. Rev.* (1970, in the press).
[2] Regge, T., and Wheeler, J. A., *Phys. Rev.*, **108**, 1903 (1957).
[3] Edelstein, L. A., and Vishveshwara, C. V., *Phys. Rev.* (1970, in the press).
[4] Edelstein, L. A., thesis, University of Maryland (1970).

Phase Change in the Upper Mantle above 350 km

BULLEN[1,2] has used the Adams-Williamson relation in region B (upper 400 km in the mantle) to relate the rate of change of density in the Earth's interior to the rate of change of seismic velocity. The Adams-Williamson relation implicitly assumed that phase changes are absent. Recent interpretations of the velocity gradient in the mantle[3] have re-emphasized the importance of phase changes in region C (between 400 and 900 km). Region B is often treated as a homogeneous layer, but I present here some evidence to show that phase change may also occur in this region.

A number of empirical equations which relate densities of common rocks and minerals with velocities of compressional waves[4-6] show that velocity is linearly proportional to density

$$V_p=A+B\rho \qquad (1)$$

where B has a value of about 3 (km/s)/(g/cm³). This relation has been applied to the calculation of density in various regions of the Earth from known seismic velocities[7-9]. For common rocks and minerals, bulk sound velocity, C, which is defined as $(V_p^2-\frac{4}{3}V_s^2)^{\frac{1}{2}}$, was also found to be linearly proportiona to density. This relation may be expressed as

$$C=a+b\rho \qquad (2)$$

where, for rocks and minerals with mean atomic weight about 21, b has a value of 2·36 (km/s)/(g/cm³) (ref. 10). This empirical relation was shown to follow closely the C versus ρ relation for a single material under large compression[11,12]. Anderson[13] gave a seismic equation of state relating the seismic parameter φ (which is identical to C^2) and ρ

$$\varphi/\varphi_0=(\rho/\rho_0)^n \qquad (3)$$

Fitting this equation to data for thirty-one selected rocks and minerals, the value for n is found to be about 3.

With increasing depth, both temperature and pressure rise. The implicit assumption in the application of any one of the empirical density velocity relations to the prediction of density in the upper mantle is that the effect of an increase of temperature and pressure with depth might change density and velocity in approximately the same ratio as that represented by the empirical relations. I have found[14] that, in regions of high temperature gradient such as the upper mantle, this assumption is violated for the relation between V_p and ρ but is obeyed for equations 2 and 3. These relations are used to estimate the density differences at various depths in the upper mantle, corresponding to a given distribution of seismic velocities.

As noted by Anderson[13], the seismic equation of state tends to predict smaller change of density than does Birch's equation of state at a given change of φ. In Fig. 1, φ/φ_0 is plotted against φ/φ_0 for the following equations: equation 6, with $b=2{\cdot}36$ (km/s)/(g/cm³) and $C_0/\rho_0=1{\cdot}8$ (km/s)/(g/cm³) as for most rocks and minerals (a is adjusted such that $C=C_0$ when $\rho=\rho_0$), equation 3 ($n=3$), and finally Birch's equation[15]

$$\varphi/\varphi_0=\tfrac{1}{2}(\rho/\rho_0)^{\frac{2}{3}}[7(\rho/\rho_0)^{\frac{2}{3}}-5] \qquad (4)$$